International Journal of Technology (2018) 6: 1187-1195
ISSN 2086-9614

PVdF-HFP QUASI-SOLID-STATE ELECTROLYTE FOR APPLICATION IN DYE-SENSITIZED SOLAR CELLS

Farish Irfal Saaid[1], Tseung-Yuen Tseng[2], Tan Winie[1,3*]

[1]*Faculty of Applied Sciences, Universiti Teknologi MARA, 40450 Shah Alam, Selangor, Malaysia*
[2]*Department of Electronics Engineering and Institute of Electronics, National Chiao-Tung University, 1001 Ta Hsueh Rd, Hsinchu 300, Taiwan*
[3]*Institute of Science, Universiti Teknologi MARA, 40450 Shah Alam, Selangor, Malaysia*

(Received: May 2018 / Revised: June 2018 / Accepted: October 2018)

ABSTRACT

A quasi-solid-state polymer electrolyte is prepared by incorporating poly(vinylidene fluoride-co-hexafluoropropylene) (PVdF-HFP) in a propylene carbonate (PC) / 1,2-dimethoxyethane (DME) / 1-methyl-3-propylimidazolium iodide (MPII) liquid electrolyte. The amount of PVdF-HFP in the liquid electrolyte is varied from 0.1 to 0.4 g. Incorporation of 0.1 g of PVdF-HFP decreases the conductivity of the DME/PC/MPII liquid electrolyte from 1.3×10^{-2} to 5.6×10^{-3} S cm^{-1}. Conductivity decreases gradually with increasing PVdF-HFP. No-flow "jelly-like" electrolyte samples are obtained for PVdF-HFP $\geq$ 0.2 g. The decrease in conductivity is the result of the decrease in ion mobility. Ion mobility was calculated by impedance spectroscopy. The PVdF-HFP quasi-solid-state electrolytes were assembled into dye sensitized solar cells (DSSCs). The performance of the DSSCs was measured under illumination of a 100 mW cm^{-2} Xenon light source. The DSSC without PVdF-HFP polymer shows an efficiency of 4.88% with short-circuit current density, J_{sc} of 11.24 mA cm^{-2}, fill factor, *FF* of 70% and open circuit voltage, V_{oc} of 619 mV. The presence of PVdF-HFP deteriorates the performance of DSSCs, but problems such as electrolyte leakage and volatilization are eliminated. The performance of DSSCs was found to be correlated to the conductivity behaviour of the electrolyte.

Keywords: Conductivity; Dye-sensitized solar cell; Ionic liquid; PVdF-HFP; Quasi-solid-state electrolyte

1. INTRODUCTION

Dye-sensitized solar cells (DSSCs) with liquid electrolytes possess high efficiencies (Fukui et al., 2006; Mathew et al., 2014). However, they suffer from leakage and electrode corrosion. Problems associated with liquid electrolytes can be eliminated by solid polymer electrolytes (SPE). But, SPE have low conductivity and poor electrolyte-electrode contact. Hence, the performance of DSSCs with SPE is poor compared to DSSC with liquid electrolytes. To overcome the shortcomings of liquid electrolytes and SPE, a quasi-solid-state electrolyte is introduced.

The quasi-solid-state electrolyte is prepared by incorporating a polymer into a liquid electrolyte. The polymer serves as a gelling agent and provides the electrolyte mechanical stability. In this work, poly(vinylidene fluoride-co-hexafluoropropylene) (PVdF-HFP) was chosen as a gelling agent for the propylene carbonate (PC) / 1,2-dimethoxyethane (DME) / 1-methyl-3-

*Corresponding author's email: tanwinie@salam.uitm.edu.my, Tel. +60-3-55444548, Fax. +60-3-55444562
Permalink/DOI: https://doi.org/10.14716/ijtech.v9i6.2344

propylimidazolium iodide (MPII) liquid electrolyte. PVdF-HFP has a high dielectric constant of 8.4 and C-F electron-withdrawing group (Sim et al., 2012), thus promoting salt dissociation. PVdF-HFP consists of crystalline VdF and amorphous HFP. The crystalline VdF offers mechanical strength whereas the amorphous HFP entraps the liquid electrolyte (Pu et al., 2006).

PVdF-HFP quasi-solid-state electrolytes were sandwiched between TiO_2 photoanode and platinum counter electrodes for DSSC assembly. This paper reports the effect of PVdF-HFP on the performance of DSSCs.

2. METHODS

2.1. Quasi-Solid-State Electrolyte Preparation and Characterization

PVdF-HFP (M_w ~4000,000 g mol^{-1}), PC, DME and MPII from Sigma-Aldrich (USA) were used as received. The liquid electrolyte was prepared by dissolving 1.0 M of MPII in PC: DME (v:v/7:3). The liquid electrolyte with 1.0 M MPII showed the highest conductivity of ~1.3×10^{-2} Scm^{-1} (Saaid et al., 2017). Different amounts of PVdF-HFP ranging from 0.1 to 0.4 g were added to the optimized liquid electrolyte and stirred at 60ºC until a "jelly-like" electrolyte was formed. The term "quasi-solid-state" is thus used to refer to the physical form of the present electrolyte that lies between a solid and a liquid state, i.e. "jelly". Viscosity profiles were measured with respect to shear rate by the Anton-Paar Physica MCR 300 rheometer (Austria). The range of shear rate was set from 0.001 to 10 s^{-1}. Electrolyte samples were sandwiched between two stainless steel plates 20 mm in diameter. All samples were rest for one minute prior to the measurements. A HIOKI 3532-50 LCR Hi-tester impedance spectrometer (Japan) was used for impedance measurement at a frequency range of 50 Hz to 1 MHz.

2.2. DSSC Fabrication and Characterization

Titanium dioxide (TiO_2) photoanode and platinum (Pt) counter electrodes were prepared according to Winie et al. (2018). The TiO_2 photoanode was immersed in 0.3 mM N719 [di-tetrabutylammonium cis-bis(isothiocyanato) bis(2,2'-bipyridyl-4,4'-dicarboxylato) ruthenium (II)] dye solution for 24 h. The dye-coated TiO_2 photoanode was then removed from the dye solution and dried at room temperature.

An amount of 0.05 g of iodine chips was added to the jelly-like electrolyte and stirred until homogeneous. For DSSC assembly, a small amount of the quasi-solid-state electrolyte was sandwiched between TiO_2 photoanode and Pt counter electrodes. The DSSC was characterized under illumination of a 100 mW cm^{-2} Xenon light (Oriel LCS 100) connected to a Metrohm Autolab potentiostat (PGSTAT128N).

3. RESULTS AND DISCUSSION

3.1. Electrolyte Characterization

Figure 1 shows the viscosity profiles with respect to shear rate for electrolyte samples with different amounts of PVdF-HFP. The Carreau model was used to fit the plots (Lam et al., 2015).

$$\frac{\eta-\eta_\infty}{\eta_0-\eta_\infty}=\left[1+(\lambda\dot{\gamma})^2\right]^{\frac{(n-1)}{2}} \quad (1)$$

where η is the viscosity at a particular shear rate, and η_0 and η_∞ are the zero-shear viscosity and infinite-shear viscosity, respectively. The time constant is λ and its value could be taken at the reciprocal value of the critical shear rate and $\dot{\gamma}_{crit}$. The flow behaviour index is given by the symbol n. The samples show a Newtonian behaviour when n = 1. The samples show a shear

thinning behaviour when $n < 1$ and a shear thickening behaviour when $n > 1$. Table 1 presents the values of η_0, η_∞, η, λ and $\dot{\gamma}_{crit}$ obtained by fitting the viscosity plots of Figure 1 with Equation 1.

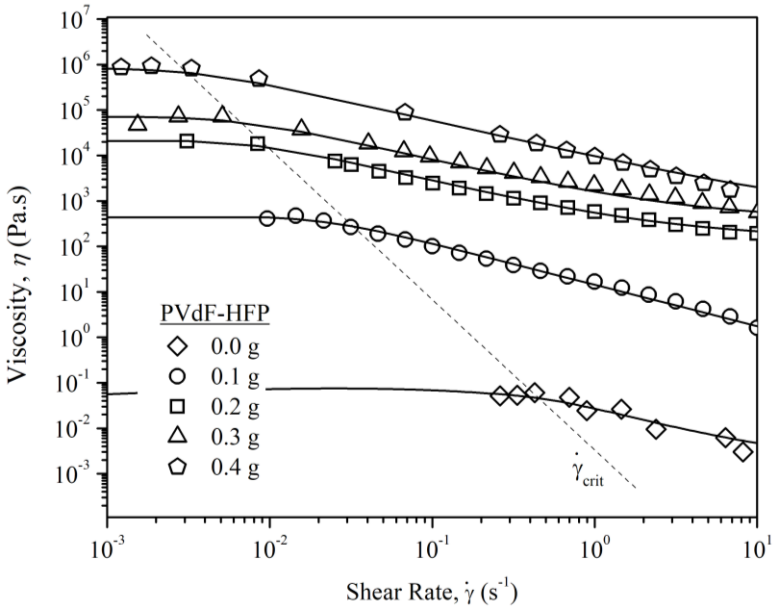

Figure 1 Plots of viscosity with respect to shear-rate for the PVdF-HFP/PC/DME/MPII electrolyte system

As observed in Table 1, all samples exhibit $n < 1$, which implies all samples show shear thinning behaviour. The value of η_0 is found to increase with increasing PVdF-HFP amounts. This indicates the electrolyte viscosity increases with PVdF-HFP. Chains of PVdF-HFP intertwist with each other. As the amount of PVdF-HFP increases, the number of intertwisted chains increase. This leads to an increase in electrolyte viscosity. On the other hand, the $\dot{\gamma}_{crit}$ decreases with increasing PVdF-HFP. The $\dot{\gamma}_{crit}$ is the transition from the viscosity plateau to the shear thinning region (Lam et al., 2015). In the shear thinning region, the rate of breakdown of the intertwisted chains exceeds the rate of formation of intertwisted chains and the electrolyte becomes less viscous. In electrolytes with more polymer molecules, the transition to the shear thinning region happens at a lower shear rate (i.e. lower $\dot{\gamma}_{crit}$) due to greater intertwisting of the polymer chains.

Table 1 The values of η_0, η_∞, n, λ and $\dot{\gamma}_{crit}$ for the PVdF-HFP/PC/DME/MPII electrolyte system

PVdF-HFP (g)	η_0 (Pa.s)	η_∞ (Pa.s)	n	λ (s)	$\dot{\gamma}_{crit}$ (s^{-1})
0.0	0.0656	0.002	0.01	2.3	0.4300
0.1	472	0.01	0.09	46.5	0.0215
0.2	22000	157	0.17	118.0	0.0085
0.3	72700	387	0.19	195.0	0.0051
0.4	980000	450	0.25	534.0	0.0019

Figure 2 shows the Nyquist plots of the prepared electrolyte samples. The plots show only steeply rising spikes. The intercept of the spike on the Z_r axis gives the value of bulk resistance, R_b. The known R_b is then used to calculate the conductivity according to:

$$\sigma = \frac{t}{R_b A} \tag{2}$$

where t is the electrolyte thickness and A is the sample-electrode contact area.

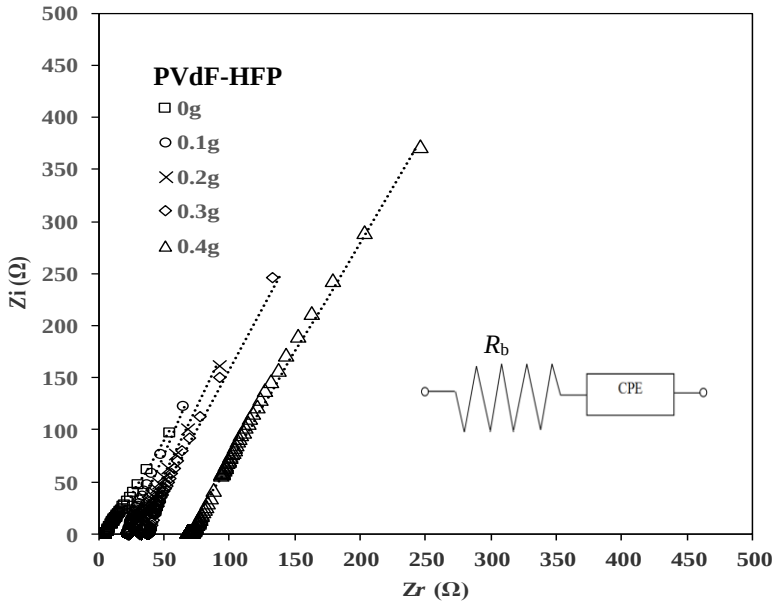

Figure 2 Room temperature Nyquist plots and their corresponding fitted lines for the PVdF-HFP/PC/DME/MPII electrolyte system. Inset: Equivalent circuit representation of Nyquist plot

The Nyquist plots in Figure 2 can be represented by a R_b connected in a series with a constant phase element (CPE) (cf. inset Figure 2). The total impedance, Z for the series combination of R_b and CPE is:

$$Z = R_b + Z_{CPE} \tag{3}$$

where the impedance of CPE is given as (Muhammad et al., 2017):

$$Z_{CPE} = \frac{1}{Qw^{\alpha}}\cos\left(\frac{\alpha\pi}{2}\right) - j\frac{1}{Qw^{\alpha}}\sin\left(\frac{\alpha\pi}{2}\right) \tag{4}$$

where Q is the capacitance of a CPE (Winie & Arof, 2014) and α is the spike deviation from the Z_r axis.

Substituting Equation 4 to Equation 3, it follows that:

$$Z = R + \frac{1}{Qw^{\alpha}}\cos\left(\frac{\alpha\pi}{2}\right) - j\frac{1}{Qw^{\alpha}}\sin\left(\frac{\alpha\pi}{2}\right) \tag{5}$$

Hence, the real Z_r and imaginary Z_i parts of the Z are:

$$Z_r = R + \frac{1}{Qw^{\alpha}}\cos\left(\frac{\alpha\pi}{2}\right) \tag{6}$$

and

$$Z_i = \frac{1}{Qw^{\alpha}} \sin\left(\frac{\alpha\pi}{2}\right) \tag{7}$$

Equations 6 and 7 are then used to fit the Nyquist plots of Figure 2 to obtain the values of Q and α. The values of Q and α are presented in Table 2.

Table 2 The values of σ, ε_r, Q, α, τ, D and μ for the PVdF-HFP/PC/DME/MPII electrolyte system

PVdF-HFP (g)	σ (S cm^{-1})	ε_r at 0.9 MHz	Q (F^{-1})	α (rad)	τ (s)	D (cm^{2}s^{-1})	μ (cm^{2}V^{-1}s^{-1})
0.0	1.3×10^{-2}	1250	1.5×10^{-4}	0.72	1.7×10^{-7}	2.8×10^{-5}	9.9×10^{-4}
0.1	5.6×10^{-3}	636	8.3×10^{-5}	0.78	3.2×10^{-7}	1.1×10^{-5}	4.2×10^{-4}
0.2	4.6×10^{-3}	390	7.7×10^{-5}	0.77	2.1×10^{-7}	7.3×10^{-6}	2.8×10^{-4}
0.3	4.1×10^{-3}	200	5.3×10^{-5}	0.74	2.0×10^{-7}	4.3×10^{-6}	1.7×10^{-4}
0.4	2.0×10^{-3}	101	4.1×10^{-5}	0.72	2.3×10^{-7}	1.6×10^{-6}	6.2×10^{-5}

The diffusion coefficient D of charge carriers developed from impedance spectroscopy is (Arof et al., 2014; Winie & Shahril, 2015):

$$D = \frac{1}{\tau}\left(\frac{\varepsilon_r \varepsilon_o A}{Q}\right)^2 \tag{8}$$

where τ is $1/\omega$. The angular frequency is ω at $Z_i \rightarrow 0$. Symbol A is the electrode-electrolyte contact area. The permittivity of free space is ε_o. The dielectric constant of the electrolyte ε_r can be obtained from the constant part of the ε_r vs. log f plot (cf. inset Figure 3).

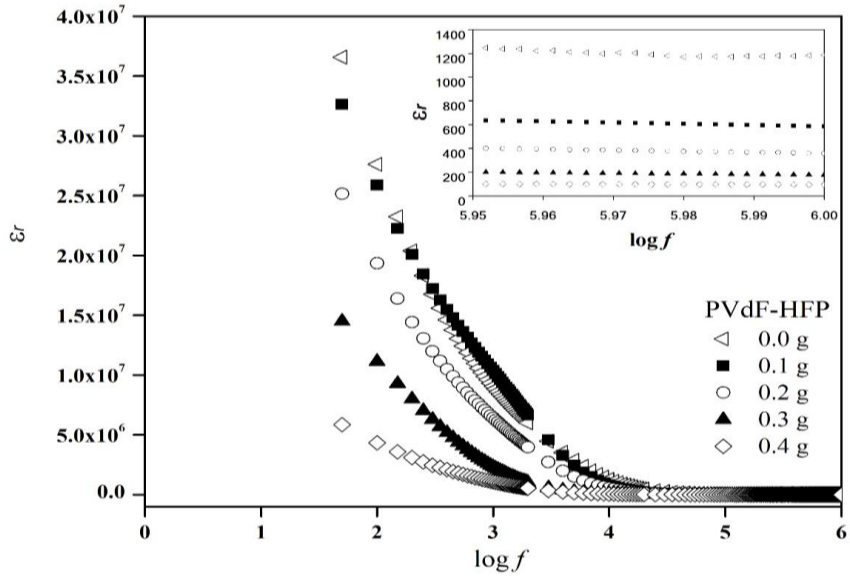

Figure 3 Plots of ε_r vs. log f for the PVdF-HFP/PC/DME/MPII electrolyte system

Knowing D, the ion mobility μ can be calculated according to the Nernst-Einstein equation (Winie & Shahril, 2015):

$$\mu = \frac{eD}{k_B T} \tag{9}$$

where e is the electronic charge, k_B is the Boltzmann constant and T is the absolute temperature in Kelvin. It is important to note that the μ is indiscriminate of speciation. Or in other words, $\mu = \mu_+ + \mu_-$, where μ_+ and μ_- are the mobility of cation and anion, respectively. Table 2 lists the calculated values of D and μ for the PVdF-HFP/PC/DME/MPII electrolyte system at room temperature.

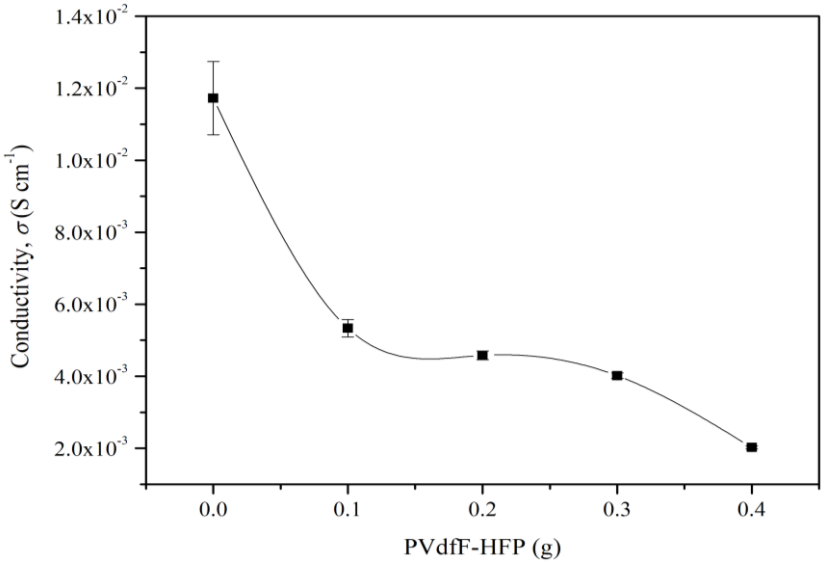

Figure 4 Room temperature conductivity with respect to PVdF-HFP amount

The variation in room temperature conductivity with respect to PVdF-HFP amount is depicted in Figure 4. The addition of 0.1 g of PVdF-HFP decreases the conductivity from 1.3×10^{-2} to 5.6×10^{-3} S cm^{-1}. Conductivity continues to decrease with the increasing PVdF-HFP amount. No-flow jelly-like electrolyte samples are obtained for PVdF-HFP $\geq$ 0.2 g. The presence of PVdF-HFP in the PC/DME/MPII liquid electrolyte provides the electrolyte mechanical stability (i.e. the ability to hold its shape) but adversely increases electrolyte viscosity (cf. Figure 1). The increase in electrolyte viscosity reduces the μ of charge carriers (cf. Table 2). A reduction in μ results in a conductivity decrement in accordance with $\sigma = en\mu$, where n is the number of ions.

3.2. DSSC Characterization

A DSSC consists of a dye-coated TiO_2 photoanode, a redox electrolyte and a Pt counter electrode. A DSSC converts light energy to electrical energy (Sofyan et al., 2017). The light-to-electricity conversion in a DSSC is based on the transfer of photo-excited electrons to the conduction band of TiO_2 and to the Pt counter electrode through the external circuit. The dye molecule absorbs the energy from the incoming photon and generates an electron-hole pair. The dye molecule becomes oxidized when the excited electron is injected into TiO_2. The I^-/I_3^- redox couple in the electrolyte is responsible for dye regeneration. The iodide ion, I^- donates an electron to the oxidized dye and becomes oxidized to triiodide, I_3^-. The triiodide ion, I_3^- recombines with the electron from the counter electrode and reduces to I^-. Then, the iodide ion, I^- releases an electron to the oxidized dye and is oxidized to I_3^- again (Nursama & Muliani, 2012). Thus, the performance of DSSC strongly depends on the transportation of iodide ions in the electrolyte.

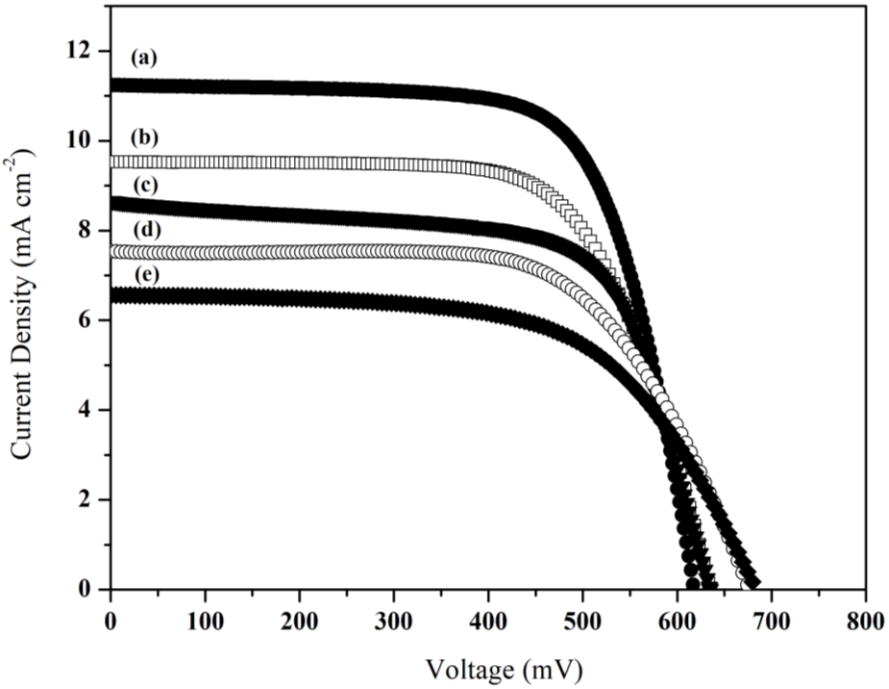

Figure 5 *J-V* curves of DSSCs for the PVdF-HFP/PC/DME/MPII electrolyte system with (a) 0.0; (b) 0.1; (c) 0.2; (d) 0.3; and (e) 0.4 g of PVdF-HFP

Figure 5 shows the *J-V* curves of DSSCs with the PVdF-HFP/PC/DME/MPII electrolyte. Their photovoltaic properties such as the open circuit voltage, V_{oc}, the short-circuit current density, J_{sc}, the fill factor, *FF* and the conversion efficiency, η are listed in Table 3. The *FF* and η were calculated using Equations 10 and 11, respectively,

$$FF = \frac{J_{\max} V_{\max}}{J_{sc} V_{oc}} \tag{10}$$

$$\eta = \frac{J_{sc} V_{oc} FF}{P_{in}} \tag{11}$$

where J_{max} and V_{max} are the current density and voltage at the maximum power output point, respectively. P_{in} is the incident light power.

Table 3 Performance parameters of DSSCs for the PVdF-HFP/PC/DME/MPII electrolyte system

PVdF-HFP (g)	V_{oc} (mV)	J_{sc} (mA cm^{-2})	*FF* (%)	η (%)
0.0	619	11.24	70	4.88
0.1	638	9.53	67	4.09
0.2	641	8.65	66	3.70
0.3	679	7.54	64	3.27
0.4	684	6.57	61	2.73

The DSSC without the PVdF-HFP polymer shows a higher η of 4.88%, J_{sc} of 11.24 mA cm^{-2}, *FF* of 70% and V_{oc} of 619 mV. The addition of 0.1 g of PVdF-HFP decreases the η to 4.09%,

the J_{sc} to 9.53 mA cm^{-2} and the *FF* to 67%. The η, J_{sc} and *FF* of the DSSCs continue to decrease with increasing polymer amounts. Conductivity due to iodide is reflected in the value of J_{sc} (Careem et al., 2017). The presence of PVdF-HFP decreases the mobility of iodide, I^- ions and hence decreases iodide conductivity (cf. Table 2). This results in a decrease in J_{sc}. On the other hand, *FF* reflects the adhesion ability of $MPIm^+$ cations on the surface of TiO_2 (Nagaraj et al., 2017). Incorporation of PVdF-HFP results in a more viscous electrolyte solution and thus reduces the mobility of $MPIm^+$ and I^-. With the reduced mobility, $MPIm^+$ cations do not move to the photoanode easily to adhere on the surface of TiO_2. Consequently, a decrease in *FF* is observed.

Adhesion of cations on the surface of TiO_2 causes surface state changes and hence shifts the Fermi level, E_F of TiO_2 towards the redox potential of I^-/I_3^- (Dissanayake et al., 2012). This means the difference between the E_F and redox potential becomes smaller and hence smaller V_{oc}. However, due to the reduced mobility in the presence of PVdF-HFP, the adhesion of $MPIm^+$ on the surface of TiO_2 decreases. Shift of E_F of TiO_2 towards the redox potential is less and this results in high value of V_{oc}. The V_{oc} of the DSSCs was observed to increase gradually as the amount of PVdF-HFP was increased. This is attributed to the gradual decrease of $MPIm^+$ mobility with PVDF-HFP (cf. Table 2).

4. CONCLUSION

The presence of PVdF-HFP in the PC/DME/MPII liquid electrolyte offers the electrolyte mechanical stability but adversely decreases electrolyte conductivity. The crystalline VdF of PVdF-HFP provides mechanical strength to the electrolyte. However, PVdF-HFP increases electrolyte viscosity and hence reduces the mobility of ions. Reduced electrolyte viscosity is evidenced from the viscosity studies. The reduction in ion mobility results in a decrease in conductivity. The DSSC assembled without PVdF-HFP shows higher efficiency than DSSCs assembled with PVdF-HFP. Although PVdF-HFP deteriorates the performance of DSSCs, it overcomes drawbacks such as electrolyte leakage and volatilization. The low conductivity of electrolytes results in low efficiency DSSCs. Thus, the conductivity of the present quasi-solid-state electrolyte needs to be further improved for application in DSSCs.

5. ACKNOWLEDGEMENT

The authors wish to thank Universiti Teknologi MARA for supporting this work through PERDANA 5/3 BESTARI (040/2018).

6. REFERENCES

Arof, A.K., Amirudin, S., Yusof, S.Z., Noor, I.M., 2014. A Method based on Impedance Spectroscopy to Determine Transport Properties of Polymer Electrolytes. *Physical Chemistry Chemical Physics*, Volume 16(5), pp. 1856–1867

Careem, M.A., Aziz, M.F., Buraidah, M.H., 2017. Boosting Efficiencies of Gel Polymer Electrolyte Based Dye. *Materials Today: Proceedings*, Volume 4(4), pp. 5092–5099

Dissanayake, M.A.K.L., Thotawatthage, C.A., Senadeera G.K.R., Bandara, T.M.W.J., Jayasundera, W.J.M.J.S.R., Mellander, B.E., 2012. Efficiency Enhancement by Mixed Cation Effect in Dye-sensitized Solar Cells with PAN Based Gel Polymer Electrolyte. *Journal of Photochemistry and Photobiology A: Chemistry*, Volume 246, pp. 29–35

Fukui, A., Komiya, R., Yamanaka, R., Islam, A., Han, L., 2006. Effect of a Redox Electrolyte in Mixed Solvents on the Photovoltaic Performance of a Dye-sensitized Solar Cell. *Solar Energy Materials and Solar Cells*, Volume 90(5), pp. 649–658

Lam, C., Martin, P.J., Jefferis, S.A., 2015. Rheological Properties of PHPA Polymer Support Fluids. *Journal of Materials in Civil Engineering*, Volume 27(11), pp. 04015021–1–04015021–9

Mathew, S., Yella, A., Gao, P., Humphry-Baker, R., Curchod, B.F., Ashari-Astani, N., Tavernelli, I., Rothlisberger, U., Nazeeruddin, M.K., Grätzel, M., 2014. Dye-sensitized Solar Cells with 13% Efficiency Achieved through the Molecular Engineering of Porphyrin Sensitizers. *Nature Chemistry*, Volume 6(3), pp. 242–247

Muhammad, F.H., Jamal, S., Winie, T., 2017. Study on Factors Governing the Conductivity Performance of Acylated Chitosan-Nai Electrolyte System. *Ionics*, Volume 23(11), pp. 3045–3056

Nagaraj, P., Sasidharan, A., David, V., Sambandam, A., 2017. Effect of Cross-linking on the Performances of Starch-based Biopolymer as Gel Electrolyte for Dye-Ssensitized Solar Cell Applications. *Polymers*, Volume 9, pp. 667–679

Nursama, N.M., Muliani, L., 2012. Investigation of Photoelectrode Materials Influences in Titania-based-Dye-sensitized Solar Cells. *International Journal of Technology*, Volume 3(2), pp. 129–139

Pu, W., He, X., Wang, L., Jiang, C., Wan, C., 2006. Preparation of PVDF–HFP Microporous Membrane for Li-ion Batteries by Phase Inversion. *Journal of Membrane Science*, Volume 272(1-2), pp. 11–14

Saaid, F., Rodi, I., Winie, T., 2017. Effect of Temperature on the Transport Property of PVdF-HFP-MPII-PC/DME Gel Polymer Electrolytes. *AIP Conference Proceedings*, Volume 1877, pp. 020006–1–020006-6

Sim, L.N., Majid, S.R., Arof, A.K., 2012, FTIR studies of PEMA/PVdF-HFP Blend Polymer Electrolyte System Incorporated with $Licf_3so_3$ Salt. *Vibrational Spectroscopy*, Volume 58, pp. 57–66

Sofyan, N., Ridhova, A., Yuwono, A.H., Udhiarto, A., 2017. Fabrication of Solar Cells with TiO_2 Nanoparticles Sensitized using Natural Dye Extracted from Mangosteen Pericarps. *International Journal of Technology*, Volume 8(7), pp. 1229–1238

Winie, T., Azmar, A., Rozana, M.D., 2018. Ionic Liquid Effect for Efficiency Improvement in Poly(methyl acrylate)/Poly(vinyl acetate)-Based Dye-sensitized Solar Cells. *High Performance Polymers*, Volume 30(8), pp. 937–948

Winie, T., Arof, A.K., 2014. *Impedance Spectroscopy: Basic Concepts and Application for Electrical Evaluation of Polymer Electrolytes*. *In*: Chan, C.H., Chia, C.H., Thomas, S. (eds.), Apple Academic Press, Inc. Canada, pp. 335–363

Winie, T., Shahril, N.S.M., 2015. Conductivity Enhancement by Controlled Percolation of Inorganic Salt in Multiphase Hexanoyl Chitosan/Polystyrene Polymer Blends. *Frontiers of Materials Science*, Volume 9(2), pp. 132–140